ARTICLE NO. 78-416R

Temperature and Heat Load Distribution in Rotating Heat Pipes

T.C. Daniels* and N.S. Al-Baharnah†
University of Swansea, Swansea, United Kingdom

An analysis is proposed for predicting the condenser wall temperature profile showing the effect of functions such as concentration of noncondensable gases, type of working fluid, condenser wall material, and cooling medium. A prediction of the heat rejected ratio of a condenser operating with noncondensable gas present to one with pure vapor is given. The working fluids considered were Arcton 113 and acetone. The noncondensable gases were nitrogen and carbon dioxide. The theoretical results obtained were checked with some experimental results using the above fluids, and an agreement was obtained.

Nomenclature

A	= cross-sectional area
C, C_1, C_2	= constants
D	= average diameter of the condenser
F	= force
G	= property group defined in Eq.(18)
L	= length of the condenser
P	= pressure
Q	= heat rate
R	= gas constant
S	= length of the gas controlled region
b	= thickness of the condenser wall
h	= heat transfer coefficient of the coolant
h_{fg}	= latent heat of evaporation
k	= thermal conductivity
m	= mass flow rate
n	= parameter defined in Eq. (3)
q	= differential heat transfer rate
r	= average radius of the condenser
t	= temperature difference
u	= condensate velocity
x,y,z	= coordinates
δ	= condensate film thickness
θ	= condenser's half-cone angle
η	= mass fraction
μ	= dynamic viscosity
ξ	= mole fraction
ρ	= density
τ	= shear force
ω	= rotational speed

Subscripts

c	= condenser
e	= operating conditions
ev	= evaporator conditions
f	= coolant conditions
g	= inert gas conditions
h	= related to the outside heat transfer coefficient
i	= interface conditions
k	= conductivity
L	= liquid phase
ℓ	= losses
o	= condenser-end conditions
r	= reference
s	= saturated (with NCG)
T	= total
v	= vapor state
w	= condenser wall conditions
z	= axial position conditions
∞	= saturation (pure vapor)

Superscripts

$( )'$	= per length
$( )^*$	= pure vapor conditions
$(\bar{})$	= average

Presented as Paper 78-416 at the AIAA Third International Heat Pipe Conference, Palo Alto, Calif., May 22-24, 1978; submitted June 23, 1978; revision received July 18, 1979.

Index categories: Heat Pipes, Heat Conduction; Thermal Control.

*Dept. of Mechanical Engineering.
†Dept. of Mechanical Engineering.

Introduction

THE work presented in this paper is a continuation of Daniels and Williams[1,2] and is concerned with the influence of noncondensable gases on the performance of a rotating heat pipe. An analysis similar to that used by Marcus and Edwards[3] is proposed for predicting the condenser wall temperature profile showing the effects of functions such as condenser wall material, cooling medium, concentration of noncondensable gases, and type of working fluid. It also predicts the heat rejected ratio of a condenser operating with noncondensable gas present to one with pure vapor only.

The assumptions used in the analysis were:

1) Film-wise condensation in the condenser.
2) Steady-state condition.
3) The flow of the condensate film is laminar.
4) An average diameter of the condenser is used.
5) The temperature distribution across the condensate film is assumed linear.
6) Velocity gradient in the circumferential direction is neglected.
7) Zero wall temperature gradient is assumed at $z = 0$.
8) The change of the condenser's cross-section area with the z-axis is neglected.
9) Axial conduction of heat by the condensate layer is neglected, compared to the axial conduction of the condenser wall.
10) Shear forces at the liquid film $y = \delta$ are neglected.
11) The latent heat is much higher than the subcooling heat.
12) The change of pressure at the liquid interface is assumed negligible since the change of the pressures of the noncondensable gas and vapor are opposite in direction.

13) The gravitational acceleration magnitude in the z and y directions is neglected since it has negative sign above and positive sign below the condenser center line.

14) The change of thickness of the liquid film layer with the z axis is much less than the half-cone angle of the condenser.

The total heat transfer to the condenser of a rotating heat pipe is mainly by the condensation process, the remainder being lost by heat conduction along the walls. This heat conduction can be obtained by considering a control volume around a differential element of the condenser, Figs. 1 and 2, and ignoring the latent heat component q.

Heat lost from the differential length dz by radiation and convection is

$$q_h = h\pi D(T_w - T_f)\,\mathrm{d}z$$

Conservation of energy around the control volume gives

$$q_z = q_{z+dz} + q_h \tag{1}$$

Neglecting the heat conducted by the condensate layer along its axial length we obtain

$$-K_c A_c \frac{\mathrm{d}T_w}{\mathrm{d}z}\bigg|_z = -K_c A_c \frac{\mathrm{d}T_w}{\mathrm{d}z}\bigg|_{z+dz} + h\pi D(T_w - T_f)\,\mathrm{d}z \tag{2}$$

where $A_c = (\pi Db)/2$. Using Taylor's expansion for $\mathrm{d}T_w/\mathrm{d}z|_{z+dz}$ and neglecting the change of the condenser's cross-sectional area with length, Eq. (2) reduces to

$$\frac{\mathrm{d}^2 t_w}{\mathrm{d}z^2} - n^2 t_w = 0 \tag{3}$$

where $t_w = T_w - T_f$ and $n^2 = 2h/k_c b$. Solving for t_w yields

$$t_w = C_1 \exp(nz) + C_2 \exp(-nz) \tag{4}$$

The boundary conditions are

$$\text{at } z=0 \quad t_w = t_0$$

$$z=L \quad t_w = t_e$$

Using the boundary conditions along with the assumption that $\exp(nL) \gg \exp(-nL)$, Eq. (4) becomes

$$t_w = t_0 \exp(-nz) + t_e\{\exp[n(z-L)] - \exp[-n(z+L)]\} \tag{5}$$

The rate of heat conduction is found by assuming that all the heat has transferred across the condenser wall cross-sectional area at $z=L$. Accordingly

$$Q_k = k_c A_c \frac{\mathrm{d}t_w}{\mathrm{d}z}\bigg|z=L \tag{6}$$

Substituting the value of t_w from Eq. (5) into Eq. (6) and neglecting higher-order terms

$$Q_k = \frac{h\pi D}{n} t_e \tag{7}$$

The heat rejected by condensation is equal to the total heat transferred minus that due to conduction and losses

$$Q = Q_T - Q_k - Q_\ell \tag{8}$$

Condenser Wall Temperature

In order to find the condenser wall temperature distribution the control volume in Fig. 2 is considered, and following the same previous analysis with the inclusion of this condensation heat flux q, we obtain

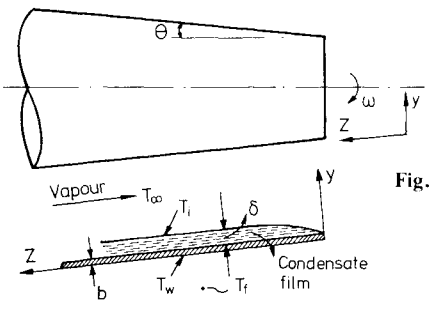

Fig. 1 Coordinate system.

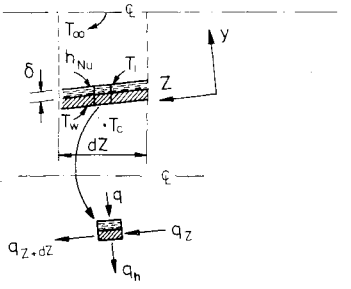

Fig. 2 Control volume.

$$\frac{\mathrm{d}^2 t_w}{\mathrm{d}z^2} = n^2 t_w - \frac{q' n^2}{h\pi D} \tag{9}$$

The boundary conditions are now

1) $z=0 \quad t_w = t_0$

2) $z=0 \quad \dfrac{\mathrm{d}t_w}{\mathrm{d}z} = 0$

3) $z=S \quad t_w = t_e$

4) $Q_T = \displaystyle\int_0^L h\pi D(T_w - T_f)\,\mathrm{d}z$

An average value of the condensation heat rate q will be taken into Eq. (9)

$$\overline{q'} = \frac{1}{L}\int_0^L q\,\mathrm{d}z \quad \therefore \quad \overline{q'} = Q/L$$

Using the preceding boundary conditions 1 and 2 above, the condenser wall temperature is

$$T_w = T_0 + C(e^{nz} + e^{-nz}) \tag{10}$$

In order to find the values of C and S the boundary conditions 3 and 4 will be used in a trial and error method. The value of the operating temperature T_0 is not yet determined. In order to find its value the saturation temperature must first be determined.

Saturation and Operating Temperatures

Consider the infinitesimal element of the condensate shown in Fig. 3 without the presence of noncondensable gas. Following the same procedure used by Daniels and Al-Jumaily[4] the sums of the forces per unit periphery are

$$\sum Fz = 0 = \frac{\partial T}{\partial y} - \frac{\partial P}{\partial z} + \rho_L \omega^2 r \sin\theta \tag{11}$$

$$\sum Fy = 0 = \frac{\partial P}{\partial y} + \rho_L \omega^2 r \cos\theta \tag{12}$$

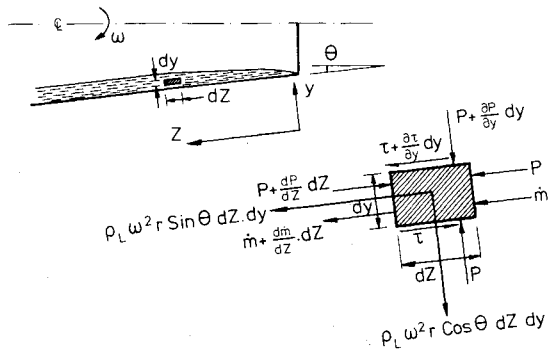

Fig. 3 Differential element in condensate layer and coordinate system.

The boundary conditions are

$$1)\ u^* = 0 \quad \text{at} \quad y = 0$$

$$2)\ \tau = \mu_L \frac{\partial u^*}{\partial y} = 0 \quad \text{at} \quad y = \delta^*$$

Integrating Eq. (12) gives

$$P = Pz - \rho_L \omega^2 r (y - \delta^*) \cos\theta$$

$$\therefore \frac{\partial P}{\partial z} = \frac{\partial Pz}{\partial z} + \rho_L \omega^2 r \cos\theta \frac{\partial \delta}{\partial z}$$

Substituting $\partial P/\partial z$ into Eq. (11) gives

$$\frac{\partial^2 u^*}{\partial y^2} = \frac{1}{\mu_L}\left(\frac{\partial Pz}{\partial z} + \rho_L \omega^2 r \cos\theta \frac{\partial \delta^*}{\partial z} - \rho_L \omega^2 r \sin\theta\right)$$

Assuming that $\mathrm{d}\delta^*/\mathrm{d}z \ll \tan\theta$ and using the second boundary condition gives

$$u^* = \frac{1}{\mu_L}\left(\frac{\partial Pz}{\partial z} - \rho_L \omega^2 r \sin\theta\right)\left(\frac{y^2}{2} - \delta^* y\right) \tag{13}$$

Assuming that the pressure P_z is constant the condensate velocity is

$$u^* = \frac{\rho_L \omega^2 r \sin\theta}{\mu_L}\left(\delta^* y - \frac{y^2}{2}\right) \tag{14}$$

The mass flow rate per unit periphery can then be obtained

$$m^* = \int_0^{\delta^*} \rho u^* \mathrm{d}y$$

Using the value of u^* from Eq. (14) in the above integral yields

$$m^* = \rho_L^2 \omega^2 r \delta^{*3} \sin\theta / 3\mu_L \tag{15}$$

The condensate heat rate q'^* is equal to

$$q'^* = k\pi D \Delta T / \delta^* \tag{16}$$

where $\Delta T = T_\infty - T_e{}^*$. The total heat condensed is equal to

$$Q^* = m^* h_{fg} \tag{17}$$

Substituting the values of δ^* and m^* from Eqs. (16) and (15) into Eq. (17) gives

$$Q^* = \frac{G^* \omega^2 r \sin\theta (\pi D)^3}{3(q^*)^3} (\Delta T)^3 \tag{18}$$

where $G^* = (\rho_L^2 k^3 h_{fg})/\mu_L$. The condensate rate q^* is assumed constant and will be equal to

$$q^* = Q^*/L \tag{19}$$

Substituting the value of q^* from Eq. (19) into Eq. (18) and rearranging, we obtain

$$\Delta T = \left[\frac{3(Q^*)^4}{G^* \omega^2 r \sin\theta (\pi D)^3 L^4}\right]^{1/3} = (T_\infty - T_e{}^*) \tag{20}$$

The operating temperature for a condenser operation with a pure vapor is constant and equal to

$$T_e^* = T_f + Q^*/(h\pi DL) \tag{21}$$

thus

$$T_\infty = T_f + \frac{Q^*}{h\pi DL} + \left(\frac{3(Q^*)^4}{G^* \omega^2 r \sin\theta (\pi D)^3 L^4}\right)^{1/3} \tag{22}$$

The property group G^* is a function of the temperature. Accordingly, Eq. (22) will be solved by a trial and error procedure for T_∞ for each given value of Q^*.

The saturated pressure is obtained by using the Clausius Clapeyron equation

$$P_\infty = P_r \exp\left[\frac{-h_{fg}}{RT_r}\left(\frac{T_r}{T_\infty} - 1\right)\right] \tag{23}$$

where T_r and P_r are reference temperature and pressure, and R the gas constant. h_{fg} is calculated at T_r and P_r. In the presence of noncondensable gas the total pressure is

$$P_T = P_g + P_\infty \tag{24}$$

where P_g is the pressure produced by the presence of a noncondensable gas (NCG). The noncondensable gas mole fraction is $\xi_g = P_g/P_T$ while the noncondensable gas mass fraction

$$\eta_g = \xi_g \Big/ \left[\xi_g + \xi_v \frac{M_v}{M_g}\right]$$

where ξ_v, M_g, and M_v are the vapor mole fraction, the noncondensable gas molecular weight, and the vapor molecular weight, respectively.

The saturation temperature is then obtained

$$T_s = T_r \Big/ \left[1 - \frac{RT_r}{h_{fg}} \ln\left(\frac{P_T}{P_r}\right)\right] \tag{25}$$

Following the same analysis as for pure vapor (Eqs. 11-20) we obtain

$$T_s = T_e + \frac{3Q^4}{G\omega^2 r \sin\theta (\pi D)^3 L^4} \tag{26}$$

Substituting Eq. (7) into Eq. (8) and neglecting the heat loss Q_ℓ we have

$$Q = Q_T - \frac{h\pi D}{n}(T_e - T_f) \tag{27}$$

Accordingly, Eqs. (26) and (27) are solved by a trial and error procedure for the operating temperature T_e.

Table 1 Dimensions for rotating pipe [1,2]

Condenser total length L	254 mm
Adiabatic section length	50 mm
Tapered half-cone angle θ	3 deg
Average outside diameter	50 mm
Thickness of condenser wall b	3 mm
Material of condenser	Copper

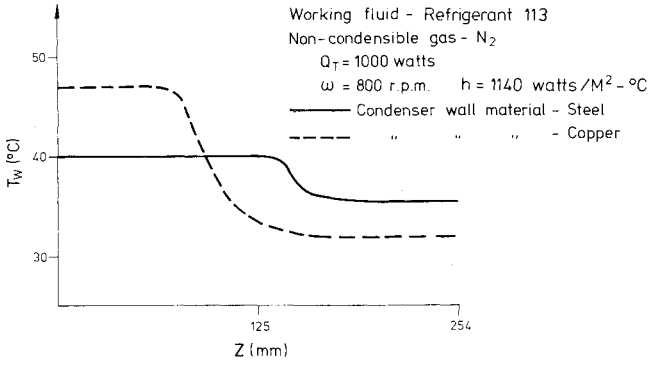

Fig. 4 Effect of condenser wall material on the wall temperature profile.

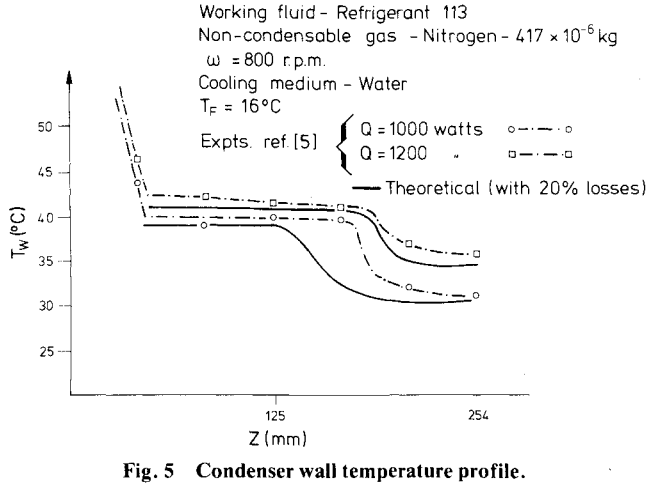

Fig. 5 Condenser wall temperature profile.

The Heat Rejected Ratio

The heat rejected ratio (HRR) for a condenser operating with NCG present to one with pure vapor only is

$$\text{HRR} = Q/Q^* \tag{28}$$

Assuming that in the pure vapor case all the heat is rejected by condensation and substituting Eq. (8) into Eq. (28) gives

$$\text{HRR} = 1 - (Q_\ell + Q_k)/Q_T$$

Theoretical Results

Theoretical results showing how the condenser wall temperature distribution is affected can now be discussed. The dimensions in Table 1 are for the rotating pipe used in Refs. 1 and 2. The working fluid properties are those for Arcton refrigerant 113 unless otherwise stated. The rotational speed, amount of NCG, outside heat transfer coefficient, and the heat input values are assumed. Accordingly, the saturation temperature and operating temperature were determined. Water was the cooling medium. (Here and after, the condenser wall temperature profile will be referred to as the temperature profile, and the HRR of a condenser operating with NCG to one with pure vapor only as the heat rejected ratio.)

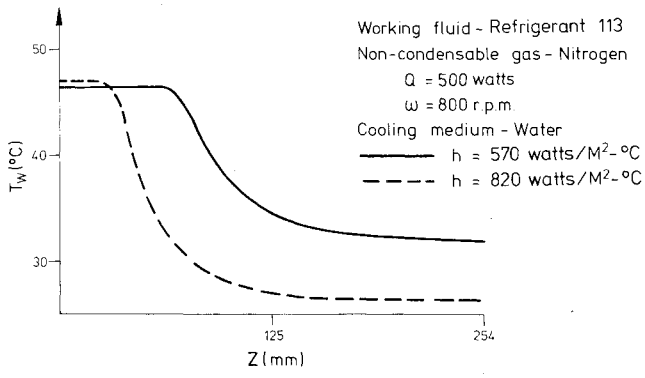

Fig. 6 Effect of the cooling medium on the temperature profile.

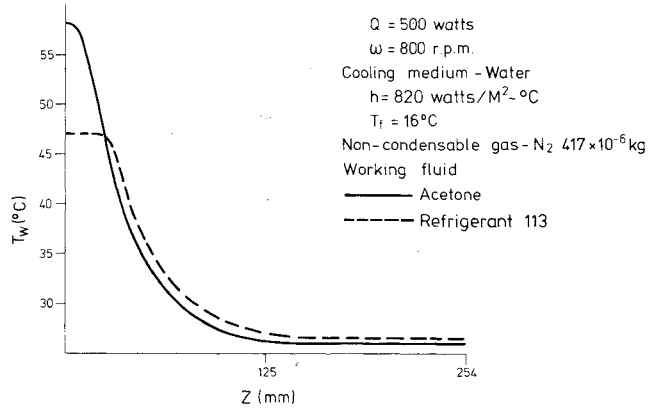

Fig. 7 Effect of the working fluid on the temperature profile.

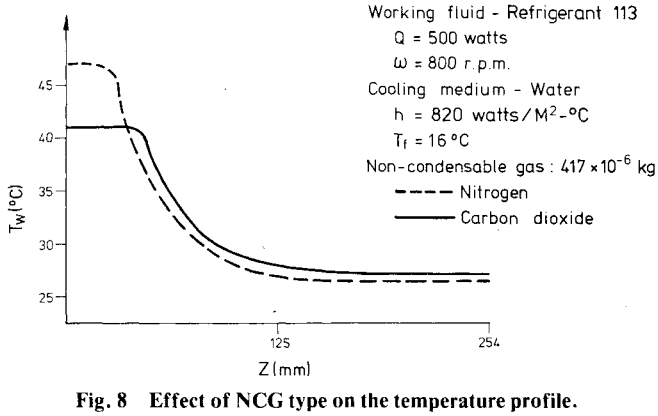

Fig. 8 Effect of NCG type on the temperature profile.

A computer program was used for solving Eqs. (22-27) for the saturation temperature T_∞ and the operating temperature T_e. Then Eq. (10) was solved for the condenser wall temperature and the length of the gas controlled region S. The temperature profile was plotted with the axial length increasing in an opposite direction to that indicated by the coordinate system in Fig. 1. Several graphs were obtained by varying only one parameter. These graphs will now be discussed in the light of factors affecting the temperature profile, and where possible direct comparison will be made with experimental evidence. The wall temperature at the evaporator starts at T_{ev}—which is higher than the saturation temperature T_s. The wall temperature then drops in the adiabatic section. This section unfortunately acts as an air-cooled precondenser due to the heat lost through the roller bearing support which could not be heat insulated. The temperature drops further to the operating temperature T_e.

The general shape of the temperature profile can be seen in Fig. 4. This shape will be approximately the same throughout.

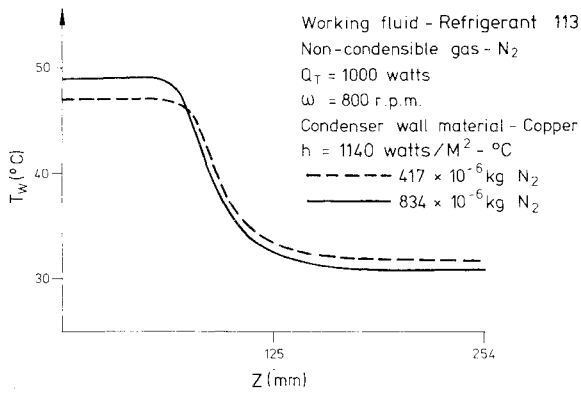

Fig. 9 Effect of the amount of noncondensable gas on the temperature profile.

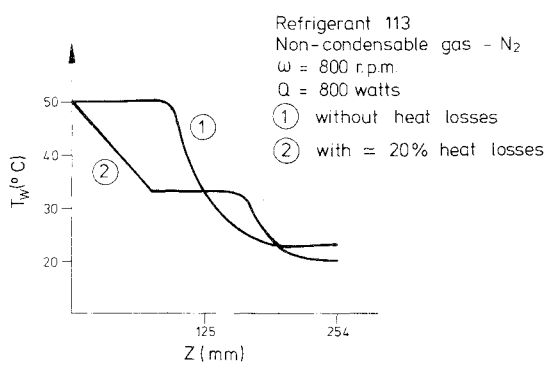

Fig. 10 Effect of heat loss on the temperature profile.

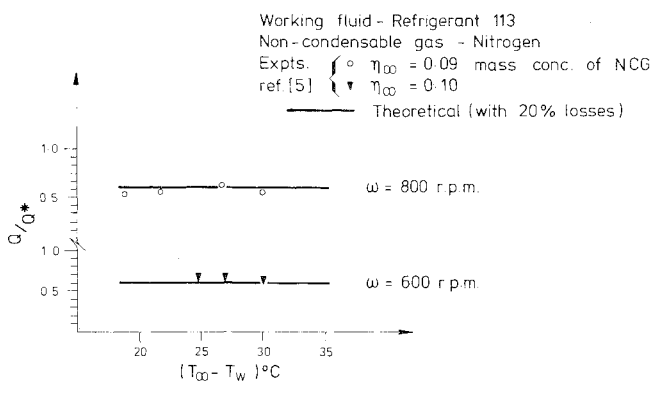

Fig. 11 Heat rejected ratio.

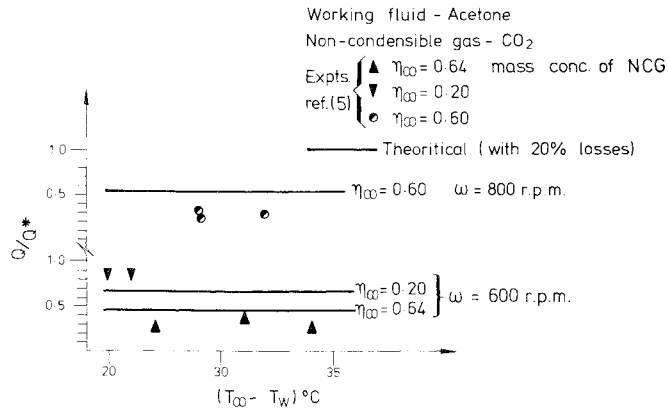

Fig. 12 Heat rejected ratio.

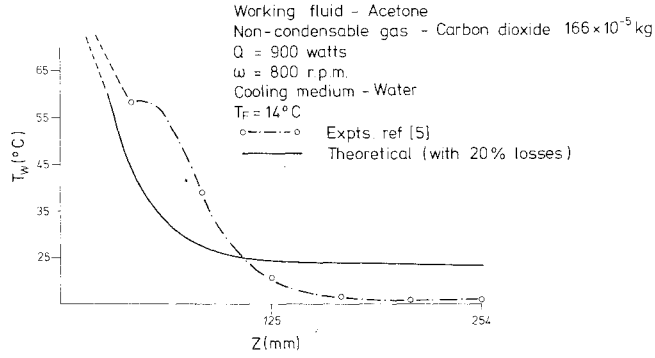

Fig. 13 Condenser wall temperature profile.

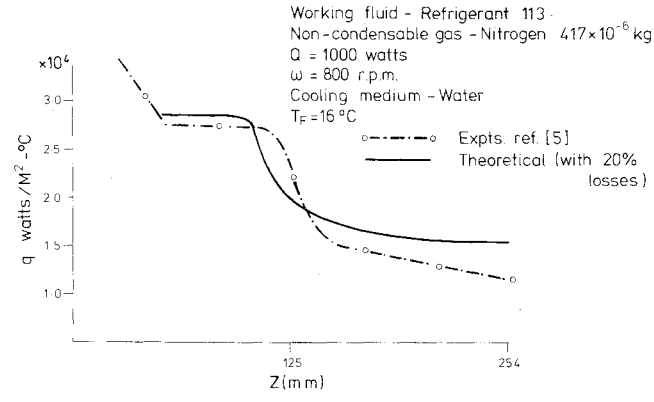

Fig. 14 Condenser heat flux profile.

The differences will be in the operating temperatures, condenser-end temperatures, the position of the curve, and its slope. The operating temperatures will be affected by the total pressure. The condenser-end temperature is directly proportional to the condensate mass flow rate times the latent heat of condensation, and inversely proportional to the cooling medium's coefficient of heat transfer. The slope of the curve depends upon the value of n in Eq. (10). The higher its value the steeper the curve. The position of the curve depends upon the amount of heat rejected.

Effect of Heat Input

The heat input is directly proportional to the total pressure in the heat pipe. Therefore, an increase in the heat input will result in an increase in total pressure; consequently, the operating temperature will increase. This results in an increase of heat conducted along the wall. The condenser-end temperature will increase due to the increase of the mass flow rate. The effect of heat input is as shown in Fig. 5.

Effect of the Cooling Medium

The effect of the cooling medium [i.e., varying the value of h in Eq. (10)] is shown in Fig. 6. It can be seen that if the outside heat transfer coefficient h is increased, the condenser-end temperature decreases and the curve is shifted toward the evaporator end. This is explained by the fact that by increasing h of the cooling medium the majority of the heat will be rejected in the part of the condenser nearest to the evaporator. A consequence of this is that the temperature has to drop rapidly to a lower level than the other curve in order to reject the rest of the heat in the remaining length of the condenser.

Effect of Condenser Wall Material

The effect of the condenser wall material, i.e., varying the value of k_c in Eq. (10), is shown in Fig. 4. Increasing the thermal conductivity of the condenser material will result in increasing the heat conducted along the condenser wall. Accordingly the heat rejected due to condensation will be less.

This will give a lower mass-flow rate, and the condenser end temperature will drop. The curve will also be flatter due to the lower tempeature gradient across the wall.

Effect of the Kind of Working Fluid

The key factor in the relation between the pressure and the temperature is the kind of fluid used. Every fluid has its own P-T relationship. Accordingly, the operating temperature will be affected by the kind of fluid used. Fig. 7 shows that for acetone the operating temperature is higher than that of Arcton 113. Therefore, for the same heat rejection, acetone will conduct more heat down the wall and lose less heat due to condensation. Consequently the mass-flow rate of acetone will be less, resulting in a lower end temperature.

Effect of Type of Noncondensable Gas Used

The equation of state for an ideal gas suggests that the pressure is inversely proportional to the molecular weight of the gas. Hence the extra pressure produced by the presence of the noncondensable gas will depend upon the gas molecular weight: the lower this value, the higher the total pressure. Figure 8 shows that the operating temperature using nitrogen as a noncondensable gas is higher than that for carbon dioxide. The condenser end temperature using nitrogen will be lower due to the higher operating temperature. Hence the heat conducted down the wall will be greater and the mass flow rate of condensate will be less, resulting in the lowering of the end temperature.

Effect of Concentration of the Noncondensable Gas

Increasing the concentration of the noncondensable gas means increasing the total pressure in the heat pipe. Therefore, the operating temperature will increase, and the condenser end temperature will decrease as illustrated in Fig. 9.

Comparison with Experimental Results

Figure 10 shows the temperature profile with and without heat losses. These losses in the adiabatic section will result in a fall in operating temperature and a shift of the curve. Throughout the comparison between theoretical and experimental results, a 20% heat loss was assumed. Three-quarters of this loss takes place in the adiabatic section and the remainder in the evaporator.

Heat Rejected Ratio

Figures 11 and 12 show a comparison of the rejected heat ratio between the experimental results (Ref. 5) and the theoretical results derived from Eq. (28) assuming 20% heat losses for Arcton 113 and acetone. A good agreement is obtained.

Temperature Profile

Figure 5 and Fig. 13 show the temperature profile comparison between theory and experiment for Arcton 113 and acetone. A reasonable agreement is obtained, and this could be improved if a more accurate value of heat losses and cooling heat transfer coefficient were obtained. Figure 14 shows a comparison between theoretical heat flux profile for Arcton 113 and the experimental results, and again a reasonable agreement is obtained.

Conclusions

The theoretical prediction seems to be substantiated when compared with existing experimental evidence. However, further experimentation is necessary to determine more accurately the heat losses extraneous to the condenser and a better value of the cooling medium's coefficient of heat transfer. Only an average value has been used in the calculations up to the present time. Variation in the condenser wall material and the taper angle should also be investigated. Work on these lines is now being pursued.

References

[1] Daniels, T.C. and Williams, R.J., "Theoretical and Experimental Analysis of Non-Condensable Gas Effects on a Rotating Heat Pipe," *Proceedings of the 2nd International Heat Pipe Conference,* Bologna, ESA Scientific and Technical Information Branch, Netherlands, 1976.

[2] Daniels, T.C. and Williams, R.J., "Experimental Temperature Distribution and Heat Load Characteristics of Rotating Heat Pipe," *International Journal of Heat Mass Transfer,* Vol. 21, 1978, p. 193-201.

[3] Edwards, D.K. and Marcus, B.D., "Heat and Mass Transfer in the Vicinity of the Vapor-Gas Front in a Gas Loaded Heat Pipe," *Journal of Heat Transfer,* Vol. C 94, May 1972, pp. 155-162.

[4] Daniels, T.C. and Al-Jumaily, F.K., "Investigations of the Factors Affecting the Performance of a Rotating Heat Pipe," *International Journal of Heat Mass Transfer,* Vol. 18, 1975, pp. 961-973.

[5] Williams, R.J., "Influence of Inert Gases on the Performance of Rotating Heat Pipes," Ph.D. thesis, University College of Swansea, Wales, UK., 1976.